MAGNETIC COILS FOR QUANTUM BIOLOGY

NANYANG TECHNOLOGICAL UNIVERSITY

Submitted
by
Zhang Wei

DIVISION OF PHYSICS & APPLIED PHYSICS
SCHOOL OF PHYSICAL AND MATHEMATICAL SCIENCES

A final year project report
presented to
Nanyang Technological University
in partial fulfilment of the
requirements for the
Bachelor of Science (Hons) in Physics
Nanyang Technological University

April 2014

Abstract

Experiments on magnetoreception of cockroaches require a large uniform magnetic field. To design a magnetic coil producing such uniform magnetic fields, we calculate and simulate the fields produced by square Helmholtz coil and the Meritt four square coil system. We find the four square coil system produces a more uniform magnetic field than the square Helmholtz coil and over much larger area. We build three four-square-coil systems so that the arbitrary magnetic field can be prepared in 3D.

Acknowledgement

I wish to thank my supervisor, Assistant Professor Tomasz Paterek, for his guidance and teaching throughout the project. I also would like to thank Dr. Agnieszka Gorecka. She explained outline of the project and guided me the design of the coil system. I would like to extend my appreciation to Mr. Abdul Rahman Bin Sulaiman for his support of constructing the coil system in Mechanical Workshop.

Contents

1 Introduction **3**

1.1 Background 3

1.2 Objective 5

1.3 Organization of the report 5

2 Future experiments that use the coil system **6**

3 Calculation and Simulation **8**

3.1 Analytical results 8

3.1.1 Helmholtz Coil 8

3.1.2 Four Square Coil System 13

4 Fabrication of magnetic coils **16**

4.1 Reason to build a 3D coil system 16

4.2 Design of the coil system 16

4.3 Construction of the coil system 20

5 Conclusion **22**

Bibiography **23**

Chapter 1

Introduction

1.1 Background

Quantum Biology Is quantum mechanics involved in biology? Do some organisms make use of quantum mechanics to gain an advantage over their competitors? Recent experiments have suggested that quantum mechanics is harnessed for a biological advantage [1]. Let us briefly give some examples.

Photosynthesis is a process used by plants and other organisms to convert light energy into chemical energy for the organisms' activities. It is a good example of quantum effects being functional in biological system. Quantum coherence is an effect in which quantum systems exist in superpositions of various states. It is a purely quantum effect, not accessible to classical systems. This effect is observed in energy transport in photosynthesis [3] [12] and allows a higher transport efficiency than in the classical models. Another indirect evidence of the presence of quantum mechanics in living organisms is the avian magnetoreception. Magnetoreception is the ability of some migrating species to navigate using the Earth's magnetic field [1]. These species utilize compass orientation controlled by the inclination compass. Earth has its geomagnetic field which generate polarity of the north and the south. The inclination compass does not rely on the polarity of the magnetic field (orientation of magnetic north) but rather on the axial direction of certain fields and its inclination [4]. There exists evidence that this compass is based on radical-pair processes in the right eye of birds [4][5]. Molecular structures in the bird's eye absorb an optical

photon and give rise to a spatially separated electron pairs in a singlet spin state which is the lowest energy state [5]. A singlet-triplet evolution occurs because of the different local environments of the two electron spins. This evolution relies on the orientation of the molecule with respect to Earth's magnetic field. The singlet and triplet electron pairs recombination leads to different chemical products whose concentration generates a chemical signal revealing information about Earth's field orientation. The inclination compass responses occur under white and low-level monochromatic light from ultraviolet to 565nm green light [4].

Magnetoreception in insects The magnetoreception has been studied in a number of diverse animal species including birds, newts, turtles etc. However, the studies on insects and other invertebrates are rare. In our experiment, we will take behavioural approach and observe insects under various magnetic conditions. Recent studies on American Cockroach show that they are sensitive to changes in magnetic field direction [2], sensitive to external radio frequency field [13]. At rest, the cockroach prefers to align with magnetic axes. The alignment is a quadrimodal alignment, that is the cockroaches align themselves perpendicularly, parallel or anti-parallel to the magnetic field. Our experiments will also the American cockroach and require a uniform magnetic field strength with spatial variation less than 2% of the field strength and direction.

Magnetic coil To determine the best magnetic coil design for the experiment, we simulate the magnetic field strength and orientation of square Helmholtz coil and four square coil system of Ref.[8]. By simulation and calculation, we find the four square coil system produces the best uniformity of the field over a large area. In our experiment, we need to change the magnetic field in 3 dimensions(see chapter 2 on experiment), thus we will build a magnetic coil to achieve this goal.

1.2 Objective

The project aims to build a magnetic coil system which produces uniform fields with spatial variation $< 2\%$ in magnitude and direction over large areas. The coil system will be used for experiments on cockroach magnetosensitivity.

1.3 Organization of the report

The report is organized as follows: The experimental methods for observing cockroach behaviour are introduced in chapter 2. Chapter 3 presents the calculations and simulations for determining the magnetic coil system of best uniformity. The procedures for fabricating the magnetic coil system are described in chapter 4. Finally, the report concludes the results of the project and suggests future works.

Chapter 2

Future experiments that use the coil system

Cockroach is chosen for the experiment because it apparently shows magnetoreception but only few studies have been done to verify this ability [2][6][10]. We would like to close this gap with emphasis on possible quantum effects and below I present two example experiments using the coils developed here that will shed more light on the magnetoreception.

Magnetoreception experiment We will install a camera to film the movements of cockroaches and count the number of body turns of the cockroaches at every time interval Δt within 1-2 hours. Only body turns more than 15° are counted. We will first conduct the experiment under Earth's magnetic field, then we will rotate the field by 60° using the coil system we build. The same experiment will be conducted under this rotated magnetic field. This experiment is an improved version of the one presented in [6], as first we would like to confirm their finding with our setup, and American cockroaches of Singapore. The improvements involve eliminating human factors, varying time intervals and measuring other parameters then the number of turns, e.g. mean path of cockroach movements.

Inclination experiment We will measure the vertical component and horizontal component of Earth's magnetic field, then vary them using the magnetic coils we build.

In this experiment we would like to follow the logic of Ref.[9]. The magnetic field will be changed while the inclination will be preserved. We then will count the number of body turn of cockroaches under different fields: inverted horizontal component, inverted vertical component and inverted both vertical and horizontal components.

Chapter 3

Calculation and Simulation

Helmholtz coil is a parallel pair of two similar size coils connected in series. The current flows in the same direction in each coil. For circular Helmholtz coil, the two coils are separated at a distance of one radius. This coil produces most uniform magnetic field.

Other than the circular Helmholtz coil, there is also square Helmholtz coil. Using the square coils instead of the circular coils might be beneficial because square coils are easier to build and the square Helmholtz coil exhibits better field-uniformity than that the field produced by the circular coils [11].

In Ref.[8], Merritt *et al.* proposed a series of coil systems including three square coil system, four square coil system and five square coil system. By calculations, they concluded four square coil system produced most uniform field. Below I present similar calculations to find the magnetic fields of both square Helmholtz coil and the four square coil system, and their arrangement giving high uniformity of the fields produced.

3.1 Analytical results

3.1.1 Helmholtz Coil

Calculation of separation between two parallel coils

The optimal separation giving most uniform field between the circular Helmholtz coil is one radius. We now derive a similar parameter for the square Helmholtz coil.

The calculation is based on Biot-Savart law. Consider the Helmholtz coil in Cartesian coordinates as shown in Figure 3.1.

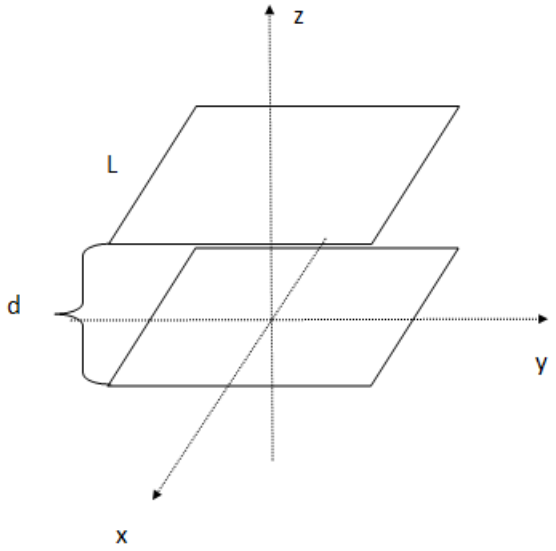

Figure 3.1: Square Helmholtz coil. The side length is L and the distance between the two coils is d

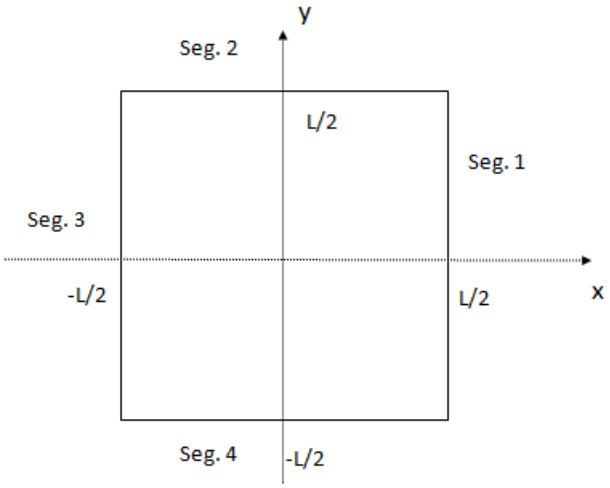

Figure 3.2: One coil of the Helmholtz coil at plane z=0

Let us divide each coil to 4 segments as presented in Figure 3.2 for the coil at plane $z = 0$. The distance vectors between an arbitrary point in 3D space $\mathbf{r} = (x, y, z)$ and an arbitrary point on the line segment $\mathbf{r'} = (x', y', z')$ for this coil is

$$\mathbf{r} - \mathbf{r'} = (x - \frac{L}{2}, y - y', z), \text{ segment 1} \tag{3.1}$$

$$\mathbf{r} - \mathbf{r'} = (x - x', y - \frac{L}{2}, z), \text{ segment 2} \tag{3.2}$$

$$\mathbf{r} - \mathbf{r'} = (x + \frac{L}{2}, y - y', z), \text{ segment 3} \tag{3.3}$$

$$\mathbf{r} - \mathbf{r'} = (x - x', y + \frac{L'}{2}, z), \text{ segment 4} \tag{3.4}$$

An infinitely small segment $d\mathbf{l}$ is

$$d\mathbf{l} = (0, dy', 0), \text{ segment 1} \tag{3.5}$$

$$d\mathbf{l} = (dx', 0, 0), \text{ segment 2} \tag{3.6}$$

$$d\mathbf{l} = (0, dy', 0), \text{ segment 3} \tag{3.7}$$

$$d\mathbf{l} = (dx', 0, 0), \text{ segment 4} \tag{3.8}$$

The calculation of the field from the coil based on Biot-Savart law, yields the results for each segment:

$$B_1 = \frac{\mu_0 I}{4\pi}\left[\int_{-\frac{L}{2}}^{\frac{L}{2}} \frac{z}{\left((y-y')^2 + \left(x - \frac{L}{2}\right)^2 + z^2\right)^{3/2}} dy'\hat{\mathbf{x}} - \int_{-\frac{L}{2}}^{\frac{L}{2}} \frac{x - \frac{L}{2}}{\left((y-y')^2 + \left(x - \frac{L}{2}\right)^2 + z^2\right)^{3/2}} dy'\hat{\mathbf{z}}\right] \tag{3.9}$$

$$B_2 = \frac{\mu_0 I}{4\pi}\left[\int_{\frac{L}{2}}^{-\frac{L}{2}} \frac{-z}{\left((y-x')^2 + \left(x - \frac{L}{2}\right)^2 + z^2\right)^{3/2}} dx'\hat{\mathbf{y}} + \int_{\frac{L}{2}}^{-\frac{L}{2}} \frac{y - \frac{L}{2}}{\left((y-x')^2 + \left(x - \frac{L}{2}\right)^2 + z^2\right)^{3/2}} dx'\hat{\mathbf{z}}\right] \tag{3.10}$$

$$B_3 = \frac{\mu_0 I}{4\pi}\left[\int_{\frac{L}{2}}^{-\frac{L}{2}} \frac{z}{\left((y-y')^2 + \left(x - \frac{L}{2}\right)^2 + z^2\right)^{3/2}} dy'\hat{\mathbf{x}} - \int_{\frac{L}{2}}^{-\frac{L}{2}} \frac{x + \frac{L}{2}}{\left((y-y')^2 + \left(x - \frac{L}{2}\right)^2 + z^2\right)^{3/2}} dy'\hat{\mathbf{z}}\right] \tag{3.11}$$

$$B_4 = \frac{\mu_0 I}{4\pi}\left[\int_{-\frac{L}{2}}^{\frac{L}{2}} -\frac{-z}{\left((x-x')^2 + \left(\frac{L}{2} + y\right)^2 + z^2\right)^{3/2}} dx'\hat{\mathbf{y}} + \int_{\frac{L}{2}}^{\frac{L}{2}} \frac{y + \frac{L}{2}}{\left((x-x')^2 + \left(y + \frac{L}{2}\right)^2 + z^2\right)^{1.5}} dx'\hat{\mathbf{z}}\right] \tag{3.12}$$

where $\hat{\mathbf{x}}$, $\hat{\mathbf{y}}$, $\hat{\mathbf{z}}$ are unit vectors in x, y and z direction.

The integrals are solved using Mathematica. The field produced by the second coil at

plane $z = d$ can be calculated by a translation of coordinates,

$$x' = x, \tag{3.13}$$

$$y' = y, \tag{3.14}$$

$$z' = z - d, \tag{3.15}$$

and using the same method as for the coil at plane $z = d$. For explicit expression for the field, see Appendix.

To find the separation d between the two coils, consider the field along z-axis,

$$B(z) = k\left(\frac{16L}{\sqrt{d^2 - 2dz + \frac{L^2}{2} + z^2}\,(4d^2 - 8dz + L^2 + 4z^2)} + \frac{8L^2}{\sqrt{\frac{L^2}{2} + z^2}\,(L^2 + 4z^2)}\right) \tag{3.16}$$

where $k = N\frac{\mu_0 I}{4\pi}$, N is the number of turns of a magnetic coil, μ_0 is the permeability of free space, $\mu_0 = 4\pi \times 10^{-7} H/m$.

Taylor expand $B(z)$ at $z = \frac{d}{2}$,

$$B(z) = B(\frac{d}{2}) + (z - \frac{d}{2})\frac{dB(z)}{dz}|_{z=\frac{d}{2}} + \frac{(z - \frac{d}{2})^2}{2}\frac{d^2B(z)}{dz^2}|_{z=\frac{d}{2}} + O(z^3) \tag{3.17}$$

To have maximum uniform field around the centre of the coil, we want more terms to be zero so that $B(z) \approx B(\frac{d}{2})$. For small z, the higher order terms are small and can be neglected. Because $B(z)$ is symmetric about $z = \frac{d}{2}$, $B(z)$ is an event function and all the odd terms vanish. For a uniform field, we choose d such that

$$\frac{d^2B(z)}{dz^2}|_{z=\frac{d}{2}} = 0 \tag{3.18}$$

The explicit calculation reveals that the second derivation at $z = \frac{d}{2}$ is:

$$\frac{d^2B(z)}{dz^2}|_{d=\frac{d}{2}} = \frac{128kL(L+2)\left(6d^6 + 18d^4L^2 + 11d^2L^4 - 5L^6\right)}{\left(d^2 + L^2\right)^3\left(d^2 + 2L^2\right)^{5/2}} \tag{3.19}$$

and accordingly the uniformity condition reveals:

$$6d^6 + 18d^4L^2 + 11d^2L^4 - 5L^6 = 0 \tag{3.20}$$

Solving the equation numerically we get

$$d = 0.5445L \tag{3.21}$$

For a coil of side length $L = 1.2$m, the separation between the coils is $d = 0.6534$m which is slightly larger than that of comparably dimensioned circular Helmholtz coils.

Plotting Magnetic Field

The field generated by the square Helmholtz coil at plane $y = 0$ is as shown in Figure 3.3. To find the uniform field with variation less than 2% at the centre, we set the limit for maximum field strength and the limit of minimum field strength, that is $99\% \times B_{centre} < B < 101\% \times B_{centre}$. By calculation using Mathematica, we find the area $\approx 0.20\text{m}^2$. Within this area the direction of the field is also uniform.

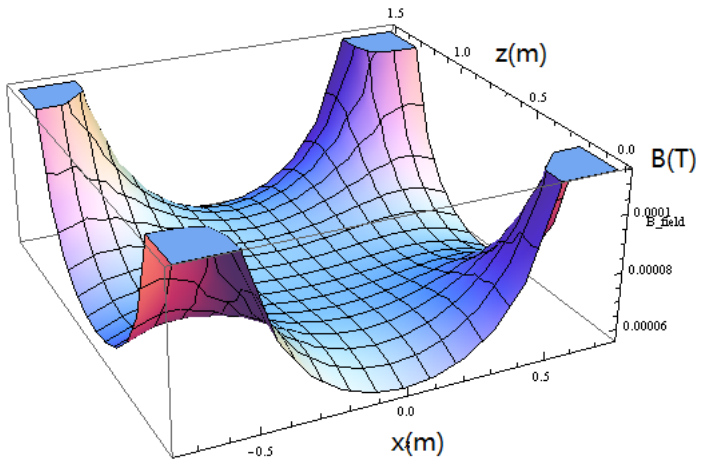

Figure 3.3: The magnetic field strength generated by square Helmholtz coil at plane $y = 0$ which is perpendicular to the coil. $L = 1.2$m, $nI = 48$A, $d = 0.6534$m, $B(T)$ indicates the magnitude of the field

We used also Radia package to verify the result. The Radia package is a 3D magnetostatics computer code based on Mathematica used to compute magnetic fields for synchrotron light sources. By plotting the field along the z axis and y axis for a square

Helmholtz coil placed symmetrically about the plane $x = 0$ and side length $L = 1.2$m, we have,

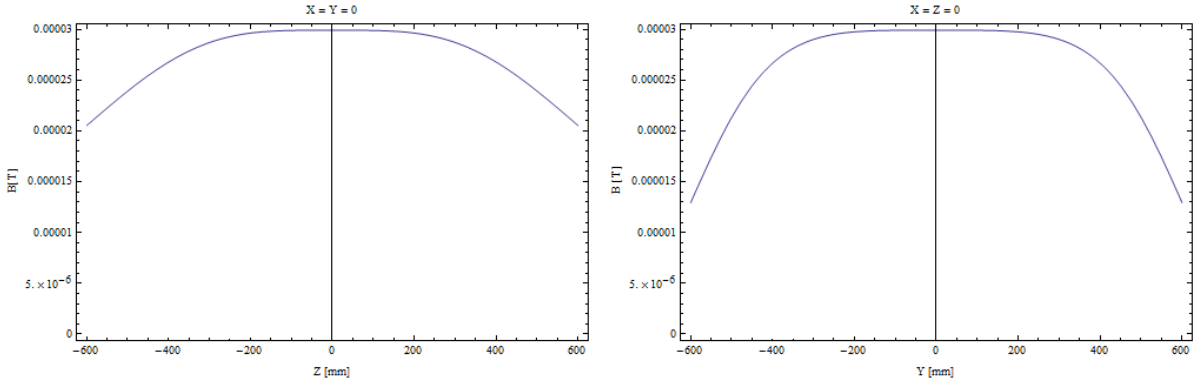

(a) (b)

Figure 3.4: (a)Magnetic field along z axis (b) Magnetic field along y axis

From Figure 3.4, we calculate the uniform field area at plane $x = 0$ of approximately $(0.42\pm0.05)\text{m}\times(0.42\pm0.05)\text{m}= 0.18\pm0.03\text{m}^2$, which agrees with previous result (0.20m^2).

3.1.2 Four Square Coil System

Calculation of the separation between four parallel coils

The four square coil system consists of four parallel coils as shown in Figure 3.5. The inner pair and outer pair of coils are placed symmetrically about plane $z = 0$

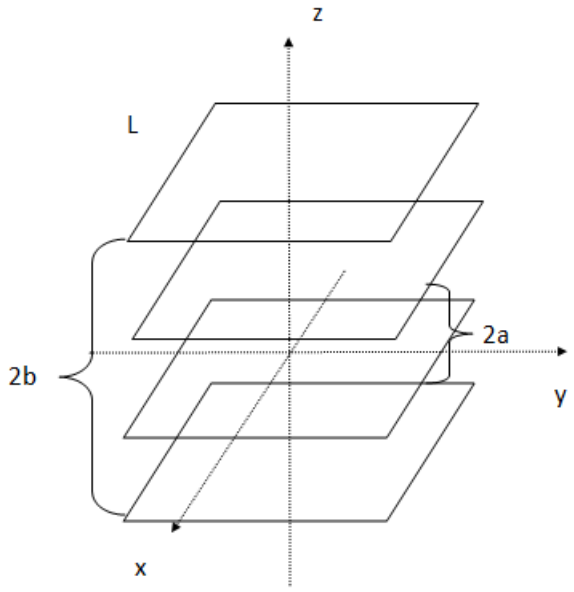

Figure 3.5: Four square coil system. The separation between inner coils is $2a$ and that between outer coils is $2b$.

We apply the same method as above to calculate the separations between the individual coils. Taylor expansion of the field along z axis to the 6th order plus elimination of the odd terms gives

$$B(z) = B(0) + \frac{(z-\frac{d}{2})^2}{2}\frac{d^2B(z)}{dz^2}|_{z=0} + \frac{(z-\frac{d}{2})^4}{4!}\frac{d^4B(z)}{dz^4}|_{z=0} + \frac{(z-\frac{d}{2})^6}{6!}\frac{d^6B(z)}{dz^6}|_{z=0} + O(z^8) \tag{3.22}$$

One can tune the parameters such that these derivatives vanish [8],

$$\frac{d^2B(z)}{dz^2} = \frac{d^4B(z)}{dz^4} = \frac{d^6B(z)}{dz^6} = 0 \tag{3.23}$$

Solving these equations, we obtain the ratio of distance a from the centre to the inner pair of coils,

$$\frac{a}{L} = 0.128106 \tag{3.24}$$

and the ratio of distance b from the centre to the outer pair of coils

$$\frac{b}{L} = 0.505492 \tag{3.25}$$

The ratio of the currents in the inner pair I' and to the order pair I is

$$\frac{I'}{I} = 0.423512 \tag{3.26}$$

Approximating the current ratio by pairs of integers, we find 11/26,25/59. We choose 11/26 as the number of turns of the inner pair and outer pair is smaller. We could have smallest number of turns winding on the coils.

Plotting Magnetic Field

Using Radia to plot the field strength along z axis and the field strength along y axis for the four coil system at plane $x = 0$ for a coil configuration as in Figure 3.5, and set the side length $L = 1.2$m. We plot Figure 3.6 and find the area of uniform field is approximated to be $(0.8 \pm 0.05\text{m}) \times (0.8 \pm 0.05\text{m}) = 0.64 \pm 0.06\text{m}^2$ (see Figure 3.6)

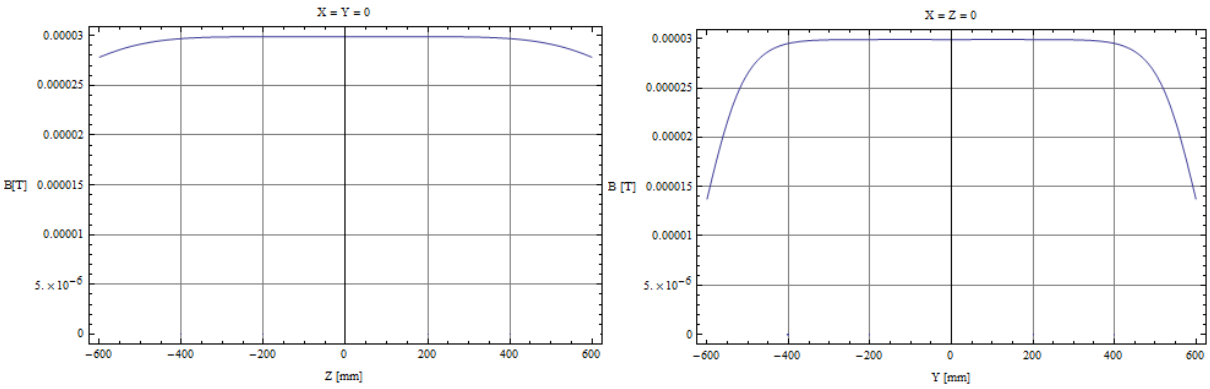

(a) (b)

Figure 3.6: (a) shows magnetic field along z axis. (b) shows magnetic field along y axis

The uniform area produced by the four square coil system is much larger than that produced by the square Helmholtz coil. Hence, we decided to fabricate a four square coil system.

Chapter 4

Fabrication of magnetic coils

4.1 Reason to build a 3D coil system

A large coil system was built because the experiments on magnetoreception require a large region of uniform magnetic field. The size of the coil is $1.2 \times 1.2 \times 1.2$ m^3.

In order to arbitrarily change the direction of the field, we need to build three four-square-coil systems of slightly different sizes so that the smaller one can be nested inside the larger. They produce a superimposed magnetic field. By altering current in one of the coil systems, we can change the field along the corresponding direction.

4.2 Design of the coil system

The prototype four coil systems is shown in Figure 4.1,

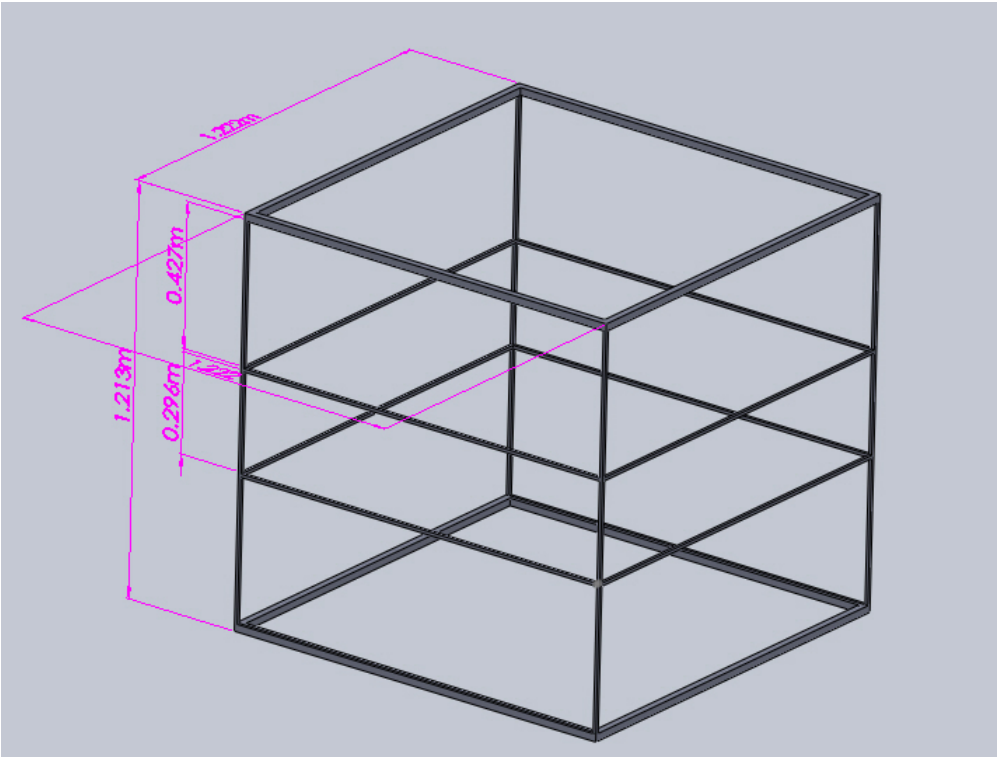

Figure 4.1: Prototype of four coil system

The separation between inner coils is 0.296m and between outer coils is 1.2m. The thickness of the thin frame is 9.8mm and that of the thick frame is 22.2mm. According to the calculation, there are 11 turns on the inner coils and 26 turns on the outer coils. The other two coil systems are similar with slightly larger sizes. The coil system in the middle between the other two has a side length of 1.278m and the largest coil system has a side length of 1.328m. The three coil systems with one inside the other are shown in Figure 4.2.

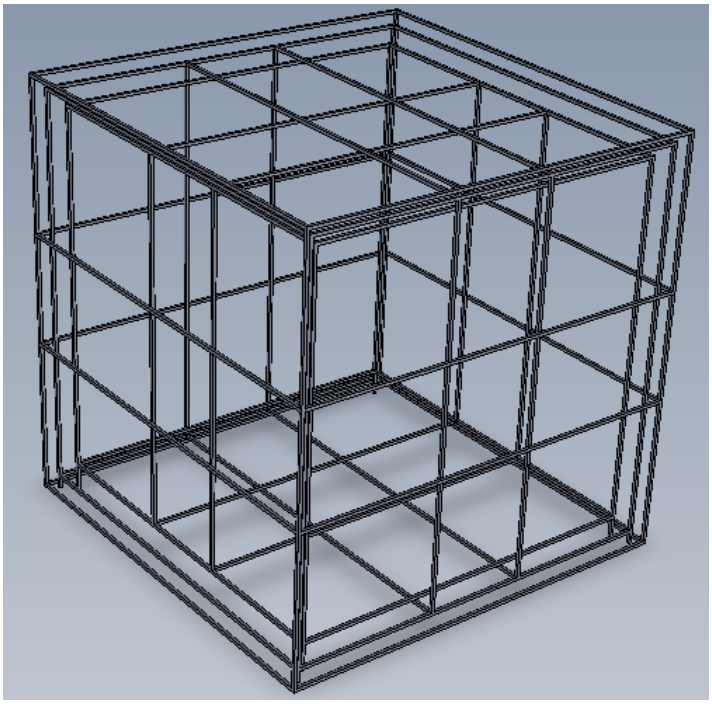

Figure 4.2: Prototype of three four-square-coil systems

Power supply By calculating and simulating the field, we need approximately 1A current in order to generate 30uT which is approximately Earth magnetic field in Singapore. The measured total resistance of the wire for one coil system is $35.1 \pm 0.1\Omega$. So the minimum power of the power supply is 35W. By carefully checking online catalogue, Agilent model E3643A and E3649A were chosen. Model E3643A is a single output DC power supply with current range 0-1.4A and power 50W. Model E3649A is a dual output power supply with current range 0-1.4A and power 100W. There are 3 power outputs in total for 3 coil systems. Both power supplies are equipped with GPIB interfaces. The GPIB (general purpose interface bus) is a digital communication bus for connecting computers and laboratory instruments so that data and control information can pass between them. The two power supplies are connected using GPIB cable (Figure 4.4(a)).

(a) (b)

Figure 4.3: (a) DC power supply, model E3643A, single output. (b) DC power supply, model E3649A, dual output

The connection between power supplies and computer is established by using USB/GPIB cable(Figure 4.4(b)). The connection is easily made by plug-and-play.

(a) (b)

Figure 4.4: (a) GPIB cable, single output. (b) USB/GPIB cable

The connections between computer, power supplies and four square coil systems are shown in Figure 4.5. The software to programme and control the power supply is Agilent

IO Libraries Suite or LabView.

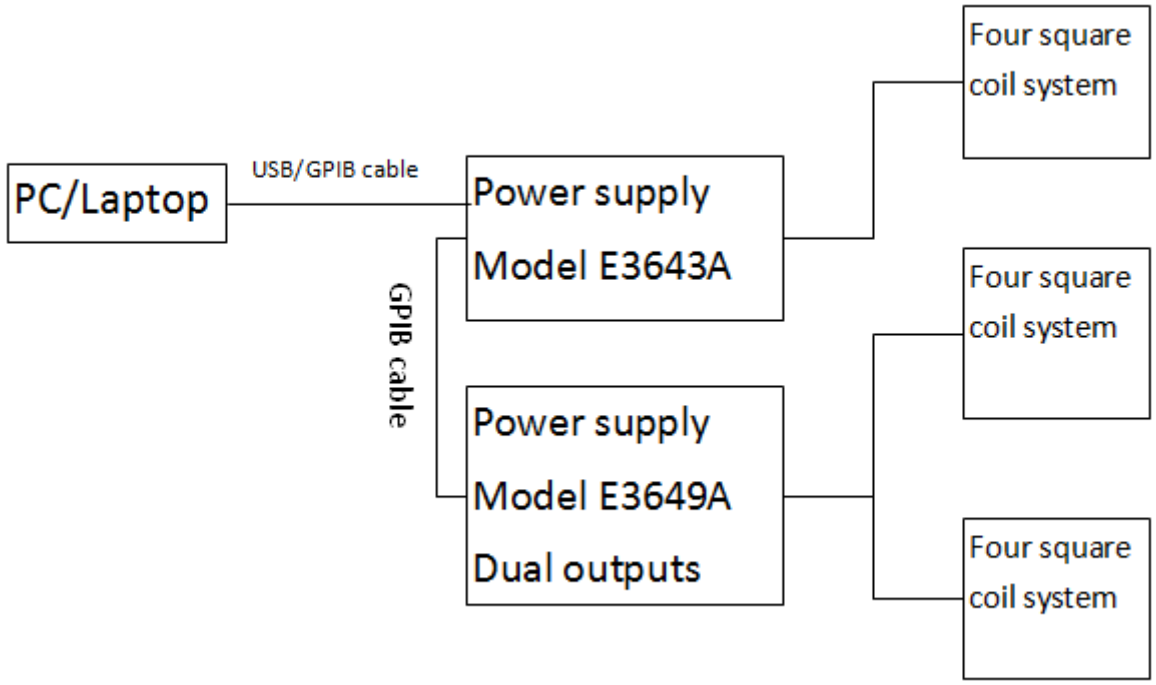

Figure 4.5: Connection between the instruments

4.3 Construction of the coil system

We choose aluminium alloy bars to construct the coil system frame. Aluminium alloy is non-magnetic under room temperature and it is largely available. The aluminium bars are also easier to cut and drill holes on.

The aluminium bars were cut into suitable lengths. Edges were filed to prevent sharp edges from cutting wires. Holes were drilled to fit screws in. The coil system was assembled as shown in Figure 4.6,

Wires used are copper wires coated with insulator. The coating of wires should be not be scratched in order to prevent shorts between wires. When winding the coils, wires were made in tension. The number of turns was checked after finishing winding by counting the number of turns directly. During winding, the wires may lose tension and come out of the frame. To keep the wire on the frame, masking tapes were used to fix the position of the wires, see Figure 4.7.

Figure 4.6: A completed four square coil system

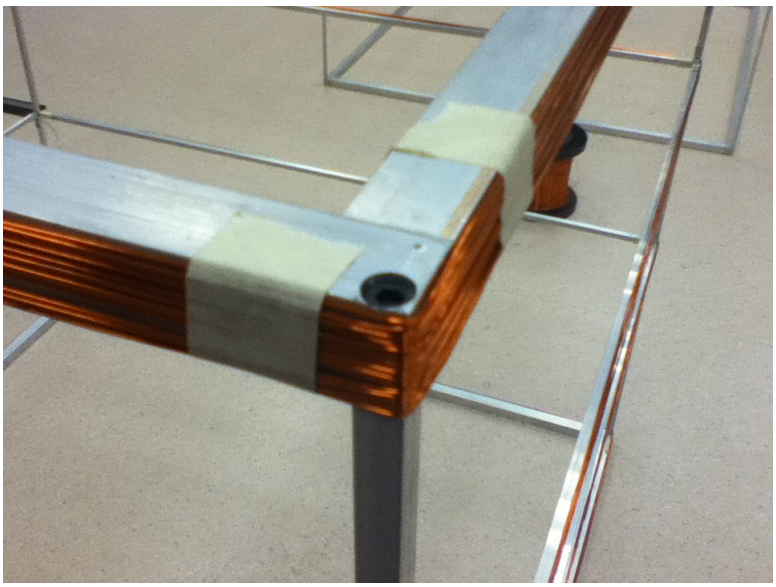

Figure 4.7: The connection of aluminium bars

Chapter 5

Conclusion

In this project, we have studied square Helmholtz coil and the four square coil system. We calculated the magnetic fields produced by both coils and simulated the fields using computer programmes. The results show the four square coil system produces about 3 times larger area of uniform magnetic field than the area produced by the square Helmholtz coil.

In the next step, we built three four-square-coil systems of slightly different sizes. The smaller one is inside the larger one so that we can change the direction of the field in 3D. Due to time constraints, the coil system has not been tested yet.

Bibliography

[1] Lambert, N., Chen, Y. N., Cheng, Y. C., Li, C. M., Chen, G. Y., Nori, F. (2013). Quantum biology. Nature Physics, 9(1), 10-18.

[2] Vácha, M. (2006). Laboratory behavioural assay of insect magnetoreception: magnetosensitivity of Periplaneta americana. Journal of experimental biology, 209(19), 3882-3886.

[3] Sarovar, M., Ishizaki, A., Fleming, G. R., Whaley, K. B. (2010). Quantum entanglement in photosynthetic light-harvesting complexes. Nature Physics, 6(6), 462-467.

[4] Wiltschko, R., Stapput, K., Thalau, P., Wiltschko, W. (2010). Directional orientation of birds by the magnetic field under different light conditions. Journal of The Royal Society Interface, 7(Suppl 2), S163-S177.

[5] Gauger, E. M., Rieper, E., Morton, J. J., Benjamin, S. C., Vedral, V. (2011). Sustained quantum coherence and entanglement in the avian compass. Physical Review Letters, 106(4), 040503.

[6] Vácha, M., Kvicalova, M., Puzova, T. (2010). American cockroaches prefer four cardinal geomagnetic positions at rest. Behaviour, 147(4), 425-440.

[7] M. Vacha, T. Puzova, M. Kvicalova. (2009) Radio frequency magnetic fields disrupt magnetoreception in American cockroach.

[8] Merritt, R., Purcell, C., Stroink, G. (1983). Uniform magnetic field produced by three, four, and five square coils. Review of Scientific Instruments, 54(7), 879-882.

[9] Wiltschko, W., Wiltschko, R. (1972). Magnetic compass of European robins. Science, 176(4030), 62-64.

[10] Vácha, M., Soukopová, H. (2004). Magnetic orientation in the mealworm beetle Tenebrio and the effect of light. Journal of experimental biology, 207(7), 1241-1248.

[11] Alamgir, A. K. M., et al. "Square Helmholtz coil with homogeneous field for magnetic measurement of longer HTS tapes." Physica C: Superconductivity 424.1 (2005): 17-24.

[12] Engel, G. S., Calhoun, T. R., Read, E. L., Ahn, T. K., Mančal, T., Cheng, Y. C., ... Fleming, G. R. (2007). Evidence for wavelike energy transfer through quantum coherence in photosynthetic systems. Nature, 446(7137), 782-786.

[13] M. Vacha, T. Puzova, M. Kvicalova. (2009) Radio frequency magnetic fields disrupt magnetoreception in American cockroach.

Appendix

The explicit result of the magnetic field produced by square Helmholtz coil, L is the side length of each individual coil and d is the separation of each individual coil.

$$
\begin{aligned}
B_x =& k\Bigg(\frac{2(L+2y)}{(4d^2-8dz+L^2+4Lx+4\left(x^2+z^2\right))\sqrt{d^2-2dz+\frac{L^2}{2}+L(x+y)+x^2+y^2+z^2}} \\
&+\frac{2(L+2y)}{(4d^2-8dz+L^2-4Lx+4\left(x^2+z^2\right))\sqrt{d^2-2dz+\frac{L^2}{2}+L(y-x)+x^2+y^2+z^2}} \\
&+\frac{2(L-2y)}{(4d^2-8dz+L^2+4Lx+4\left(x^2+z^2\right))\sqrt{d^2-2dz+\frac{L^2}{2}+L(x-y)+x^2+y^2+z^2}} \\
&+\frac{2(L-2y)}{(4d^2-8dz+L^2-4Lx+4\left(x^2+z^2\right))\sqrt{d^2-2dz+\frac{L^2}{2}-L(x+y)+x^2+y^2+z^2}} \\
&+z\Bigg(-\frac{2(L+2y)}{(L^2+4Lx+4\left(x^2+z^2\right))\sqrt{\frac{L^2}{2}+L(x+y)+x^2+y^2+z^2}} \\
&-\frac{2(L-2y)}{(L^2+4Lx+4\left(x^2+z^2\right))\sqrt{\frac{L^2}{2}+L(x-y)+x^2+y^2+z^2}}\Bigg) \\
&+z\Bigg(\frac{2(L+2y)}{(L^2-4Lx+4\left(x^2+z^2\right))\sqrt{\frac{L^2}{2}+L(y-x)+x^2+y^2+z^2}} \\
&+\frac{2(L-2y)}{(L^2-4Lx+4\left(x^2+z^2\right))\sqrt{\frac{L^2}{2}-L(x+y)+x^2+y^2+z^2}}\Bigg)\Bigg)
\end{aligned}
\tag{5.1}
$$

where $k = \frac{u_0 I}{4\pi}$

$$
\begin{aligned}
B_y =& k\Bigg(\frac{2(L+2x)}{(4d^2-8dz+L^2+4Ly+4\left(y^2+z^2\right))\sqrt{d^2-2dz+\frac{L^2}{2}+L(x+y)+x^2+y^2+z^2}} \\
&+\frac{2(L+2x)}{(4d^2-8dz+L^2-4Ly+4\left(y^2+z^2\right))\sqrt{d^2-2dz+\frac{L^2}{2}+L(x-y)+x^2+y^2+z^2}} \\
&+\frac{2(L-2x)}{(4d^2-8dz+L^2+4Ly+4\left(y^2+z^2\right))\sqrt{d^2-2dz+\frac{L^2}{2}+L(y-x)+x^2+y^2+z^2}} \\
&+\frac{2(L-2x)}{(4d^2-8dz+L^2-4Ly+4\left(y^2+z^2\right))\sqrt{d^2-2dz+\frac{L^2}{2}-L(x+y)+x^2+y^2+z^2}} \\
&-z\Bigg(\frac{2(L+2x)}{(L^2+4Ly+4\left(y^2+z^2\right))\sqrt{\frac{L^2}{2}+L(x+y)+x^2+y^2+z^2}} \\
&+\frac{2(L-2x)}{(L^2+4Ly+4\left(y^2+z^2\right))\sqrt{\frac{L^2}{2}+L(y-x)+x^2+y^2+z^2}}\Bigg) \\
&-z\Bigg(-\frac{2(L+2x)}{(L^2-4Ly+4\left(y^2+z^2\right))\sqrt{\frac{L^2}{2}+L(x-y)+x^2+y^2+z^2}} \\
&-\frac{2(L-2x)}{(L^2-4Ly+4\left(y^2+z^2\right))\sqrt{\frac{L^2}{2}-L(x+y)+x^2+y^2+z^2}}\Bigg)\Bigg)
\end{aligned}
\tag{5.2}
$$

$$
\begin{aligned}
B_z =& k\Bigg(\frac{(L-2y)(L+2x)}{\sqrt{\frac{L^2}{2}+(x-y)L+x^2+y^2+z^2}\,(L^2+4xL+4\,(x^2+z^2))} \\
&+\frac{(L+2y)(L+2x)}{\sqrt{\frac{L^2}{2}+(x+y)L+x^2+y^2+z^2}\,(L^2+4xL+4\,(x^2+z^2))} \\
&+\frac{(L+2y)(L+2x)}{\sqrt{\frac{L^2}{2}+(x+y)L+x^2+y^2+z^2}\,(L^2+4yL+4\,(y^2+z^2))} \\
&+\frac{(L-2y)(L+2x)}{\sqrt{\frac{L^2}{2}+(x-y)L+x^2+y^2+z^2}\,(L^2-4yL+4\,(y^2+z^2))} \\
&+\frac{2(L+2x)}{\sqrt{d^2-2zd+\frac{L^2}{2}+x^2+y^2+z^2+L(x+y)}\,(4d^2-8zd+L^2+4Ly+4\,(y^2+z^2))} \\
&+\frac{2(L+2x)}{\sqrt{d^2-2zd+\frac{L^2}{2}+x^2+y^2+z^2+L(x-y)}\,(4d^2-8zd+L^2-4Ly+4\,(y^2+z^2))} \\
&+\frac{(L-2x)(L+2y)}{\sqrt{\frac{L^2}{2}+(y-x)L+x^2+y^2+z^2}\,(L^2-4xL+4\,(x^2+z^2))} \\
&+\frac{(L-2x)(L-2y)}{\sqrt{\frac{L^2}{2}-(x+y)L+x^2+y^2+z^2}\,(L^2-4xL+4\,(x^2+z^2))} \\
&+\frac{2(L-2y)}{\sqrt{d^2-2zd+\frac{L^2}{2}+x^2+y^2+z^2+L(x-y)}\,(4d^2-8zd+L^2+4Lx+4\,(x^2+z^2))} \\
&+\frac{2(L+2y)}{\sqrt{d^2-2zd+\frac{L^2}{2}+x^2+y^2+z^2+L(x+y)}\,(4d^2-8zd+L^2+4Lx+4\,(x^2+z^2))} \\
&+\frac{2(L+2y)}{\sqrt{d^2-2zd+\frac{L^2}{2}+x^2+y^2+z^2+L(y-x)}\,(4d^2-8zd+L^2-4Lx+4\,(x^2+z^2))} \\
&+\frac{2(L-2y)}{\sqrt{d^2-2zd+\frac{L^2}{2}+x^2+y^2+z^2-L(x+y)}\,(4d^2-8zd+L^2-4Lx+4\,(x^2+z^2))} \\
&+\frac{(L-2x)(L+2y)}{\sqrt{\frac{L^2}{2}+(y-x)L+x^2+y^2+z^2}\,(L^2+4yL+4\,(y^2+z^2))} \\
&+\frac{(L-2x)(L-2y)}{\sqrt{\frac{L^2}{2}-(x+y)L+x^2+y^2+z^2}\,(L^2-4yL+4\,(y^2+z^2))} \\
&+\frac{2(L-2x)}{\sqrt{d^2-2zd+\frac{L^2}{2}+x^2+y^2+z^2+L(y-x)}\,(4d^2-8zd+L^2+4Ly+4\,(y^2+z^2))} \\
&+\frac{2(L-2x)}{\sqrt{d^2-2zd+\frac{L^2}{2}+x^2+y^2+z^2-L(x+y)}\,(4d^2-8zd+L^2-4Ly+4\,(y^2+z^2))}\Bigg)
\end{aligned}
\tag{5.3}
$$

Mathematica code of Radia package to calculate the magnetic field.

For square Helmholtz coil

```
<<Radia‘;
RadUtiMem[];
j1=26;j2=j1*0.423514;
n1=3;c2={1,0,0};c1={0,1,1};thcn=0.001;
Rt1=radObjRaceTrk[{0.,0.,653.4/2},{1,1.7},{1200.,1200.},1,n1,j1];
radObjDrwAtr[Rt1,c1,thcn];

Grp=radObjCnt[{Rt1}];
RadTrfZerPara[Grp,{0,0,0},{0,0,1}];
dr=radObjDrw[Grp];
Show[Graphics3D[dr]]

Plot[radFld[Grp,"h",{0,0,z}],{z,-600,600}
,AxesOrigin->{0,0}
,FrameLabel->{"Z [mm]","B[T]","X = Y = 0",""}]

Plot[radFld[Grp,"h",{0,y,0}],{y,-600,600}
,AxesOrigin->{0,0}
,FrameLabel->{"Y [mm]","B [T]","X = Z = 0",""}]
```

For the four square coil system

```
<<Radia‘;
RadUtiMem[];
j1=3.6;j2=j1*0.423514;
n1=3;c2={1,0,0};c1={0,1,1};thcn=0.001;
Rt1=radObjRaceTrk[{0.,0.,153.7272},{1,4.56},{1200.,1200.},1,n1,j2];
```

```
radObjDrwAtr[Rt1,c1,thcn];
Rt2=radObjRaceTrk[{0.,0.,606.5904},{1,4.56},{1200.,1200.},1,n1,j1];
radObjDrwAtr[Rt2,c1,thcn];
Grp=radObjCnt[{Rt1,Rt2}];
RadTrfZerPara[Grp,{0,0,0},{0,0,1}];
dr=radObjDrw[Grp];
Show[Graphics3D[dr]]
Plot[radFld[Grp,"h",{0,0,z}],{z,-600,600}
,AxesOrigin->{0,0}
,FrameLabel->{"Z [mm]","B[T]","X = Y = 0",""}]

Plot[radFld[Grp,"h",{0,y,0}],{y,-600,600}
,AxesOrigin->{0,0}
,FrameLabel->{"Y [mm]","B [T]","X = Z = 0",""}]
radFldUnits[]
```